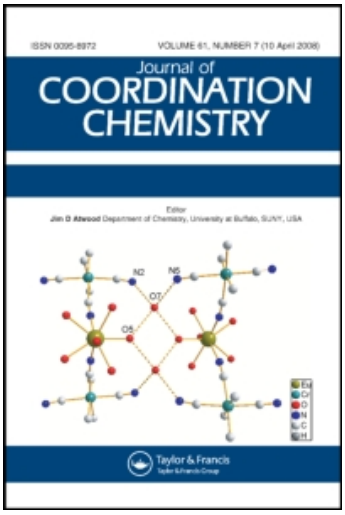

Journal of Coordination Chemistry
Publication details, including instructions for authors and subscription information:
http://www.informaworld.com/smpp/title~content=t713455674

Two new polyoxometalate-based organic-inorganic hybrids: synthesis, crystal structure and characterization

Wei-Lin Chen[a]; Yong-Hui Wang[a]; Yang-Guang Li[a]; En-Bo Wang[a]; Yun-Wu Li[a]
[a] Key Laboratory of Polyoxometalate Science of Ministry of Education, Department of Chemistry, Institute of Polyoxometalate Chemistry, Northeast Normal University, Changchun, Jilin 130024, P.R. China

First published on: 29 July 2010

To cite this Article Chen, Wei-Lin , Wang, Yong-Hui , Li, Yang-Guang , Wang, En-Bo and Li, Yun-Wu(2009) 'Two new polyoxometalate-based organic-inorganic hybrids: synthesis, crystal structure and characterization', Journal of Coordination Chemistry, 62: 7, 1035 — 1050, First published on: 29 July 2010 (iFirst)
To link to this Article: DOI: 10.1080/00958970802401097
URL: http://dx.doi.org/10.1080/00958970802401097

Journal of Coordination Chemistry
Vol. 62, No. 7, 10 April 2009, 1035–1050

Taylor & Francis
Taylor & Francis Group

Two new polyoxometalate-based organic-inorganic hybrids: synthesis, crystal structure and characterization

WEI-LIN CHEN, YONG-HUI WANG, YANG-GUANG LI*, EN-BO WANG* and YUN-WU LI

Key Laboratory of Polyoxometalate Science of Ministry of Education, Department of Chemistry, Institute of Polyoxometalate Chemistry, Northeast Normal University, Changchun, Jilin 130024, P.R. China

(*Received 12 May 2008; in final form 23 June 2008*)

Two new organic-inorganic hybrids, (4,4′-bipy)[Cu^{I}(2,2′-bipy)$_2$]$_2$[W_6O_{19}] (2,2′-bipy = 2,2′-bipyrine, 4,4′-bipy = 4,4′-bipyrine) (**1**) and ($C_6H_5NO_2$)$_4${Mn^{III}(H_2O)}[$As^{III}W_9O_{33}$]$_2${W(OH)}-{W(H_2O)}•~18H_2O (**2**), have been synthesized and characterized by elemental analysis, IR, TG, UV–Vis, XRPD, XPS, electrochemical analysis and single-crystal X-ray diffraction. Single crystal X-ray diffraction analysis shows that **1** is a new Lindqvist-type polyoxoanion bisupported by copper(I) coordination cations and 2,2′-bipy ligands and exhibits a three-dimensional (3-D) supermolecular framework by aromatic π–π stacking interactions. Compound **2** is constructed from a manganese(III)-substituted sandwich-type polyoxoanion based on [α-AsW_9O_{33}]$^{9-}$ units and dissociative, protonated pyridine-4-carboxylic acid molecules, which act as the charge compensation cations. The cyclic voltammogram of **2** shows an irreversible redox process for Mn^{3+} ions.

Keywords: Polyoxometalate; Organic-inorganic hybrid; π–π Stacking interaction; Lindqvist; Sandwich-type

1. Introduction

Design and construction of organic-inorganic hybrid materials with structural diversity, fascinating properties, and potential applications in catalysis, molecular adsorption, medicine, electro-conductivity, magnetism and photochemistry have been one of the focuses of recent research [1]. The evolution of organic-inorganic hybrid materials is dependent upon the synthesis of new solids possessing unique structures and properties. In this area, polyoxometalates (POMs) with versatile structural topologies and nucleophilic oxygen-enriched surfaces represent one of the excellent inorganic multi-dentate O-donor ligands [2]. One promising strategy to construct new organic-inorganic hybrid materials is to connect POM building units with secondary transition metal complexes or lanthanide complexes via covalent bonds [3]. The transition metal (TM)

*Corresponding authors. Email: wangenbo@public.cc.jl.cn; liyg658@nenu.edu.cn

ISSN 0095-8972 print/ISSN 1029-0389 online © 2009 Taylor & Francis
DOI: 10.1080/00958970802401097

complexes dramatically influence the inorganic oxide microstructure by providing charge compensation and/or becoming a part of the inorganic POM framework. To realize a controllable synthesis, it is very important to select proper POM building blocks and interesting TM complexes as modifiers [4].

Commonly used POM building blocks still largely focus on Keggin-, Wells-Dawson-[5] and Anderson-type polyoxoanions [6], as well as some isopolyoxoanions [7]. A number of examples of new hybrid solids containing such POM units include $(NH_4)[Cu_{24}I_{10}L_{12}][PMo_2^{V}Mo_{10}^{VI}O_{40}]_3$ (L = 4-[3-(1H-1,2,4-triazol-1-yl)propyl]-4H-1,2,4-triazole [5d], $[\{La(DMF)_6(H_2O)\}\{La(DMF)_{4.5}(H_2O)_{2.5}\}(P_2W_{18}O_{62})]$ [5h], $[Cu_2(bpy)_2(\mu\text{-ox})][Cr(OH)_7Mo_6O_{17}]$ [6a], $[Cu^{II}(2,2'\text{-bipy})(H_2O)_2Al(OH)_6Mo_6O_{18}]_n^{n-}$ [6b], $[Cu_3^{I}Cl(4,4'\text{-bipy})_4][Cu^{II}(1,10\text{-phen})_2Mo_8O_{26}]$ [7b], $(Hapy)_4[Co(H_2O)_5Mo_7O_{24}]\cdot 9H_2O$ (apy = 2-aminopyridine) [7c], $[Cd(BPE)(\alpha\text{-}Mo_8O_{26})][Cd(BPE)(DMF)_4]\cdot 2DMF$ (BPE = 1,2-*bis*(4-pyridyl)ethane, DMF = *N*,*N*-dimethylformamide) [7d]. However, organic-inorganic hybrid materials based on Lindqvist-type POMs or sandwich-type polyoxoanions have been less reported. Sandwich-type polyoxoanions, as a large subfamily of transition-metal-substituted POMs, have larger volumes and more negative charges than commonly used POMs, allowing formation of higher coordination numbers with metal cations. Thus, both kinds of polyoxoanions should be excellent precursors for constructing organic-inorganic hybrids. Only a few examples have been reported [8], such as $[Cu(4,4'\text{-bipy})]\{[Cu(4,4'\text{-bipy})]_2[W_6O_{19}]\}\cdot 4H_2O$ [5c], $[Co_2(bpy)_6(W_6O_{19})_2]$ [8a], $[Cu^{II}(H_2O)_4(\text{dibenzo-24-crown-8}][Mo_6^{VI}O_{19}]$ [8b], $\{[(en)Pd(4,4'\text{-bpy})]_4[W_6O_{19}]\}(NO_3)_6$ [8c], $(n\text{Bu}_4\text{N})_2[NbW_5O_{19}SiRR'_2]$ (R = R′ = Et, *i*Pr, O*t*Bu, Ph; R = *t*Bu and R′ = Me) [8d], $\{Nb_6O_{19}[Cu(2,2'\text{-bipy})]_2[Cu(2,2'\text{-bipy})_2]_2\}\cdot 19H_2O$ [8e], $[Cu(dien)(H_2O)]_2\{[Cu(dien)(H_2O)]_2\ [Cu(dien)(H_2O)_2]_2[Cu_4(SiW_9O_{34})_2]\}\cdot 5H_2O$ [3c], and $[\{Ni_7(\mu_3\text{-}OH)_3O_2(dap)_3(H_2O)_6\}(B\text{-}\alpha\text{-}PW_9O_{34})]$ $[\{Ni_6(\mu_3\text{-}OH)_3(dap)_3(H_2O)_6\}(B\text{-}\alpha\text{-}PW_9O_{34})][Ni(dap)_2(H_2O)_2]\cdot 4.5H_2O$ (dap = 1,2-diaminopropane) [3b]. Therefore, it is still a current challenge to explore suitable synthetic conditions to obtain this kind of hybrid compound.

Here we report two new organic-inorganic hybrid materials based on two kinds of POM building blocks, $(4,4'\text{-bipy})[Cu^{I}(2,2'\text{-bipy})_2]_2[W_6O_{19}]$ (2,2′-bipy = 2,2′-bipyrine, 4,4′-bipy = 4,4′-bipyrine) (**1**) and $(C_6H_5NO_2)_4\{Mn^{III}(H_2O)\}[As^{III}W_9O_{33}]_2\{W(OH)\}\{W(H_2O)\}\bullet\sim 18H_2O$ (**2**). Compound **1** is a new Lindqvist-type polyoxoanion bisupported by copper(I) coordination cations and the 2,2′-bipy ligands, and thus a 3-D supermolecular framework is formed via aromatic π–π stacking interactions. Compound **2** is constructed from a high-valent manganese-substituted sandwich-type POM based on $[\alpha\text{-}AsW_9O_{33}]^{9-}$ units and dissociative, protonated pyridine-4-carboxylic acid molecules acting as the charge compensation cations. Synthesis of $Mn^{III/IV}$-substituted POMs is usually difficult owing to the higher instability of these ions in aqueous solution compared with other transition metal ions.

2. Experimental

2.1. *Materials*

All chemicals were commercially purchased and used without purification. $Na_9[AsW_9O_{33}]\bullet\sim 19.5H_2O$ was synthesized according to the literature method [9].

2.2. *Synthesis of complexes*

2.2.1. (4,4′-bipy)[Cu^{I}(2,2′-bipy)$_2$]$_2$[W_6O_{19}] (1). A mixture of $Na_2WO_4 \cdot 2H_2O$ (3.30 g, 10 mmol), $CuSO_4 \cdot 5H_2O$ (0.125 g, 0.5 mmol), 4,4′-bipy (0.23 g, 1.5 mmol), 2,2′-bipy (0.234 g, 1.5 mmol), Na_2VO_3 (0.75 mmol, 0.12 g) and H_2O (12 mL) was stirred for half an hour in air. Then the pH was adjusted to 5.22 by 6 M hydrochloric acid and the mixture transferred to a Teflon-lined autoclave (23 mL) and kept at 170°C for five days. After the autoclave was slowly cooled to room temperature, green crystals were filtered off, washed with distilled water and dried in a desiccator at room temperature (yield 46% based on W). Elemental analysis for $C_{50}H_{40}Cu_2N_{10}O_{19}W_6$ (**1**) Calcd C, 25.94; H, 1.74; N, 6.05; Cu, 5.49; W, 47.65 (%); found: C, 25.90; H, 1.69; N, 6.01; Cu, 5.52; W, 47.62 (%).

2.2.2. ($C_6H_5NO_2$)$_4${$Mn^{III}(H_2O)$}[$As^{III}W_9O_{33}$]$_2${W(OH)}{$W(H_2O)$}•∼18H_2O (2). To a 20-mL aqueous solution of $Na_9[AsW_9O_{33}]\bullet\sim 19.5H_2O$ (2.63 g, 1 mmol) was added dropwise an aqueous solution prepared by dissolving $MnCl_2 \cdot 4H_2O$ (0.297 g, 1.5 mmol) and pyridine-4-carboxylic acid (0.246 g, 2 mmol) at the same time in 15 mL of distilled water. Then $K_2S_2O_8$ (0.15 g, 0.5 mmol) was added with stirring, the solution was adjusted to pH = 2.0 by addition of 1 mol L^{-1} KOH and refluxed for 2 h during which the color changed from orange to red-brown. After cooling to room temperature, the yellow suspension was filtered and the filtrate was kept at room temperature. Brown columnar crystals of **2** were isolated after ten days (yield 60% based on W). Elemental analysis for $C_{24}H_{61}As_2MnN_4O_{95}W_{20}$ (**2**) Calcd C, 4.96; H, 1.06; N, 0.96; Mn, 0.95; W, 63.31 (%); found: C, 4.92; H, 1.01; N, 0.90; Mn, 0.97; W, 63.27 (%).

2.3. *Physical measurements*

Elemental analyses of W and Cu were performed by a Leaman inductively coupled plasma (ICP) spectrometer; C and N were performed on a Perkin–Elmer 2400 CHN elemental analyzer. FT-IR spectra were recorded from 400–4000 cm^{-1} on an Alpha Centauri FT-IR spectrophotometer using KBr pellets. TG analyses were performed on a Perkin–Elmer TGA7 instrument in flowing N_2 with a heating rate of 10°C min^{-1}. XPS analyses were performed on a VG ESCALABMKII spectrometer with a Mg–Kα (1253.6 eV) achromatic X-ray source. The vacuum inside the analysis chamber was maintained at 6.2×10^{-6} Pa during the analysis. Diffuse reflectance UV–Vis spectrum for **1** ($BaSO_4$ pellet) was obtained with a Varian Cary 500 UV–vis NIR spectrometer. UV–Vis absorption spectra for **2** were obtained using a 752 PC UV–Vis spectrophotometer. X-ray powder diffractometry (XRPD) studies were performed with a NETZSCH STA 449C instrument including a Panalytical X-Pert pro diffractometer with Cu–Kα radiation. Electrochemical measurements were carried out on a CHI 660A electrochemical workstation at room temperature (25–30°C) under nitrogen. A pHS-25B type pH meter was used for pH measurement.

2.4. *Electrochemical experiment*

A CHI 600 electrochemical workstation connected to a Pentium-IV personal computer was used for control of the electrochemical measurements and for data collection.

Table 1. Crystal data and structure refinements for **1** and **2**.

Complex	**1**	**2**
Chemical formula	$C_{50}H_{40}Cu_2N_{10}O_{19}W_6$	$C_{24}H_{61}As_2MnN_4O_{95}W_{20}$
Formula weight (M)	2315.06	5807.55
Temperature (K)	293(2)	150(2)
Wavelength (Å)	0.71073	0.71073
Crystal system	Triclinic	Monoclinic
Space group	$P\bar{1}$	$P2(1)/n$
Unit cell dimensions (Å, °)		
a	10.614(2)	16.846(3)
b	11.067(2)	23.625(5)
c	12.626(3)	29.308(6)
α	73.71(3)	90
β	77.70(3)	91.37(3)
γ	71.37(3)	90
V (Å^3)	1336.5(5)	11661(4)
Z	1	4
D_{Calcd} (g cm^{-3})	2.876	3.308
μ (Mo-Kα) (mm^{-1})	13.720	20.408
$F(000)$	1064	10256
Goodness-of-fit on F^2	1.041	0.950
R_1^a	0.0764	0.0708
wR_2^b	0.2262	0.1499
R_1 (all data)	0.0838	0.1689
wR_2 (all data)	0.2329	0.1917

[a] $R_1 = \Sigma\|F_o| - |F_c\|/\Sigma|F_o|$. [b] $wR_2 = \Sigma[w(F_o^2 - F_c^2)^2]/\Sigma[w(F_o^2)^2]^{1/2}$.

A conventional three-electrode system was used. The working electrode was glassy carbon. A Ag/AgCl electrode was used as the reference electrode and platinum wire as a counter electrode. The scan rate was 10 mV s^{-1}. All potentials were measured and reported *versus* the Ag/AgCl. All the experiments were conducted at room temperature (25–30°C). Cyclic voltammogram of **2** was recorded on 1 mM solutions in 0.5 M H_2SO_4/Na_2SO_4 at pH = 2.0.

2.5. *Single-crystal X-ray diffraction*

Single crystals of **1** of size 0.28 × 0.26 × 0.22 mm and **2** of 0.25 × 0.23 × 0.21 mm were mounted on glass fibers. The crystallographic data were collected at 293 K for **1** and 150 K for **2** on a Rigaku R-axis Rapid IP diffractometer using graphite monochromatic Mo-Kα radiation (λ = 0.71073 Å) operating at 50 kV and 200 mA with IP technique. Data processing was accomplished with the RAXWISH processing program. Empirical absorption correction was applied. A total of 10090 reflections for **1** were collected, of which 4485 reflections were unique; a total of 82616 reflections for **2** were collected, of which 20348 were unique. The structures of **1** and **2** were solved by the direct method and refined by full-matrix least-squares method on F^2 using the SHELXTL-97 crystallographic software package [10]. During the refinement of **1**, anisotropic thermal parameters were used to refine all non-hydrogen atoms. Carbon-bound hydrogen atoms were placed in geometrically calculated positions with the use of a riding model and refined with fixed isotropic thermal parameters.

During refinement of **2**, there are a number of short connections between OW(water) ... O(POM) in the range of 2.60 ~ 2.90 Å, suggesting extensive H-bonding interactions

between lattice water molecules and the polyanions. However, the H atoms between them cannot be determined from the difference Fourier maps due to the limited quality of the data. All H atoms on water molecules were directly included in the molecular formula. In **2**, only partial lattice water molecules can be accurately assigned from the residual electron peaks, while the rest were directly included in the molecular formula based on elemental and TG analyses. The W19, Mn2 and W21 sites are size-occupancy disordered with the occupancies of 80% (20%) for W19 (Mn1), 60% (40%) for W20 (Mn2), and 60% (40%) for W21 (Mn3), respectively. Also, two of the five pyridine-4-carboxylic acid molecules are disordered with occupancies of 50%. So the polyanion in **2** is charge-balanced by four protonated pyridine-4-carboxylic acid molecules. Further details of the X-ray structural analysis of **1** and **2** are provided in table 1. Selected bond lengths and angles of **1** and **2** are listed in tables S1–S2, respectively.

3. Results and discussion

3.1. *Synthesis*

The successful isolation of **1** depends on the exploitation of hydrothermal technique. Hydrothermal synthesis has proved to be a particularly useful technique in preparation of organic-inorganic hybrid materials [11]. The exploitation of hydrothermal conditions requires a shift in paradigm from the thermodynamic to the kinetic so that equilibrium phases are replaced by structurally more complex metastable phases [12]. Hydrothermal synthesis is still a relatively complex process because many factors can influence the outcome of a reaction, such as the type of initial reactants, starting concentrations, pH values, reaction time and temperature [13].

Compound **1** was separated from the hydrothermal reaction of $Na_2WO_4 \cdot 2H_2O$, $CuSO_4 \cdot 5H_2O$, 4,4′-bipy, 2,2′-bipy, Na_2VO_3 and H_2O at 170°C and pH 5.22 for five days. Parallel experiments showed that the pH value of the reaction system was crucial for the crystallization. Green crystals of **1** could only be obtained in the pH range of 5.0–5.5. Within the pH range of 3.0–5.0, no crystalline phase was formed and the product was a mixture of brown and black powders. In addition, the nature of the transition metal is also important for the formation of **1**. We tried to replace $CuSO_4 \cdot 5H_2O$ with $CoSO_4 \cdot 7H_2O$ or $ZnSO_4 \cdot 7H_2O$ in the synthetic process, but no isostructural compounds were obtained.

The temperature may be another crucial factor for the isolation of **1**. If the reaction temperature is lower than 170°C, no crystals could be obtained. It is noteworthy that if Na_2VO_3 was not introduced into the reaction mixture, no compound is isolated under similar reaction conditions ($T = 170$°C and pH = 5.22). Thus, it is supposed that Na_2VO_3 is necessary for the preparation of **1**. Also, it may act as a reducing agent to reduce the Cu^{2+}.

Most POM-based clusters have been prepared by a "step-by-step" building-block approach. This synthetic process is also involved in the formation of lacunary polyoxoanion building blocks. In the synthesis of **2**, we use $[\alpha\text{-}AsW_9O_{33}]^{9-}$ as the precursor. The crucial factors for the preparation of **2** may be the pH value of the reaction system and the use of the superfluous pyridine-4-carboxylic acid. A series of parallel synthetic experiments indicate that **2** can be isolated in a broad pH range of $1.0 \sim 3.5$. At higher pH values from 4.5 to 5.5,

$Na_{8.25}[\{Mn^{III}(H_2O)\}_{2.25}(WO(H_2O))_{0.75}(AsW_9O_{33})_2] \cdot 28H_2O$ [14] was synthesized. When the pH was above 5.5, no crystalline phase was formed and the product was yellow suspensions. The introduction of this reactant prevents the coordination of K or Na cations to the sandwich-type polyoxoanions and may serve as useful precursors in future syntheses. In the sandwiching position of **2**, there is enough space to accommodate other metal cations (see figure 4). In the following experiments, we will use **2** as a precursor to react with other transition metals or lanthanide cations in order to obtain the heteronuclear clusters on the basis of POMs. During the reaction, the color of the solution changed from orange to red brown, indicating that the Mn^{2+} cations were oxidized to Mn^{3+}.

3.2. *Structure description*

Single-crystal X-ray diffraction analysis reveals that **1** is composed of one $[W_6O_{19}]^{2-}$ anion decorated with two $[Cu^{I}(2,2'\text{-bipy})_2]^{2-}$ units and one 4,4′-bipy molecule (see figure 1). In the polyoxoanion of **1**, the classical Lindqvist-type polyoxoanion $[W_6O_{19}]^{2-}$ is built up from six distorted WO_6 edge-shared octahedra [see figure 1(b)]. All W centers exhibit a hexa-coordinate environment with W–O bond lengths in the range 1.686(13) ~ 2.3121(12) Å and O–W–O bond angles varying from 76.5(4) to 179.3(5)° (see table S1).

In the two $[Cu^{I}(2,2'\text{-bipy})_2]^{2-}$ units of **1**, there is only one crystallographically independent copper Cu(1), which coordinates directly to the surface of the polyoxoanion. Cu(1) is five-coordinate, defined by four nitrogen atoms from 2,2′-bipy and one bridging oxygen O(3) from the polyoxoanion, but not the adjacent terminal oxygen atoms [O(10) and O(9A)]. The Cu(1)–O(3) bond length is 2.017(13) Å and Cu–N is in the range 1.969(18)~2.104(18) Å (see table S1). The $[W_6O_{19}]^{2-}$ polyoxoanion is supported by two $[Cu^{I}(2,2'\text{-bipy})_2]^{2-}$ units via the bridging oxygen atoms of the polyoxoanion [see figure 1(a)]. Frameworks based on Lindqvist-type polyoxoanions are less reported. In **1**, all W and Cu centers exhibit the +6 and +1 oxidation states, respectively, based on their coordination environments, bond lengths and angles and the bond valence sum BVS calculations [15].

The most unusual structural feature of **1** is that the $[Cu^{I}(2,2'\text{-bipy})_2]^{2-}$ units are joined together by aromatic π–π stacking interactions so that **1** exhibits an interesting 3-D supramolecular framework as shown in figures 2, 3 and S1. From the packing view of **1** along the *a* axis, open cavities can be observed in which the 4,4′-bipy molecules exist (see figure 2). Along the *b* and *c* axes, **1** also displays two different but interesting views (see figures 3 and S1).

Single crystal X-ray diffraction analysis shows that the polyanion of **2** consists of two $[\alpha\text{-}AsW_9O_{33}]^{9-}$ moieties linked by one {W(OH)}, one $\{W(H_2O)\}$ and one $\{Mn^{III}(H_2O)\}$ units via the W–O–M (M=W or Mn) connection mode, leading to a sandwich-type structure (see figures 4 and S2). The W–O bond lengths are in the range 1.655(16)~2.344(19) Å and O–W–O bond angles vary from 86.0(8) to 175.4(8)° (see table S2). All W and Mn sites in the central sandwiched part exhibit a square-pyramidal penta-coordinate environment. Furthermore, these three metal centers are disordered, that is, the {W(OH)}, $\{W(H_2O)\}$ and $\{Mn^{III}(H_2O)\}$ units share the three parts with the occupancies of 80% in W19, 60% in W21 and 40% in Mn2 site, respectively (see figures 4 and S2). It is interesting that there are no potassium or

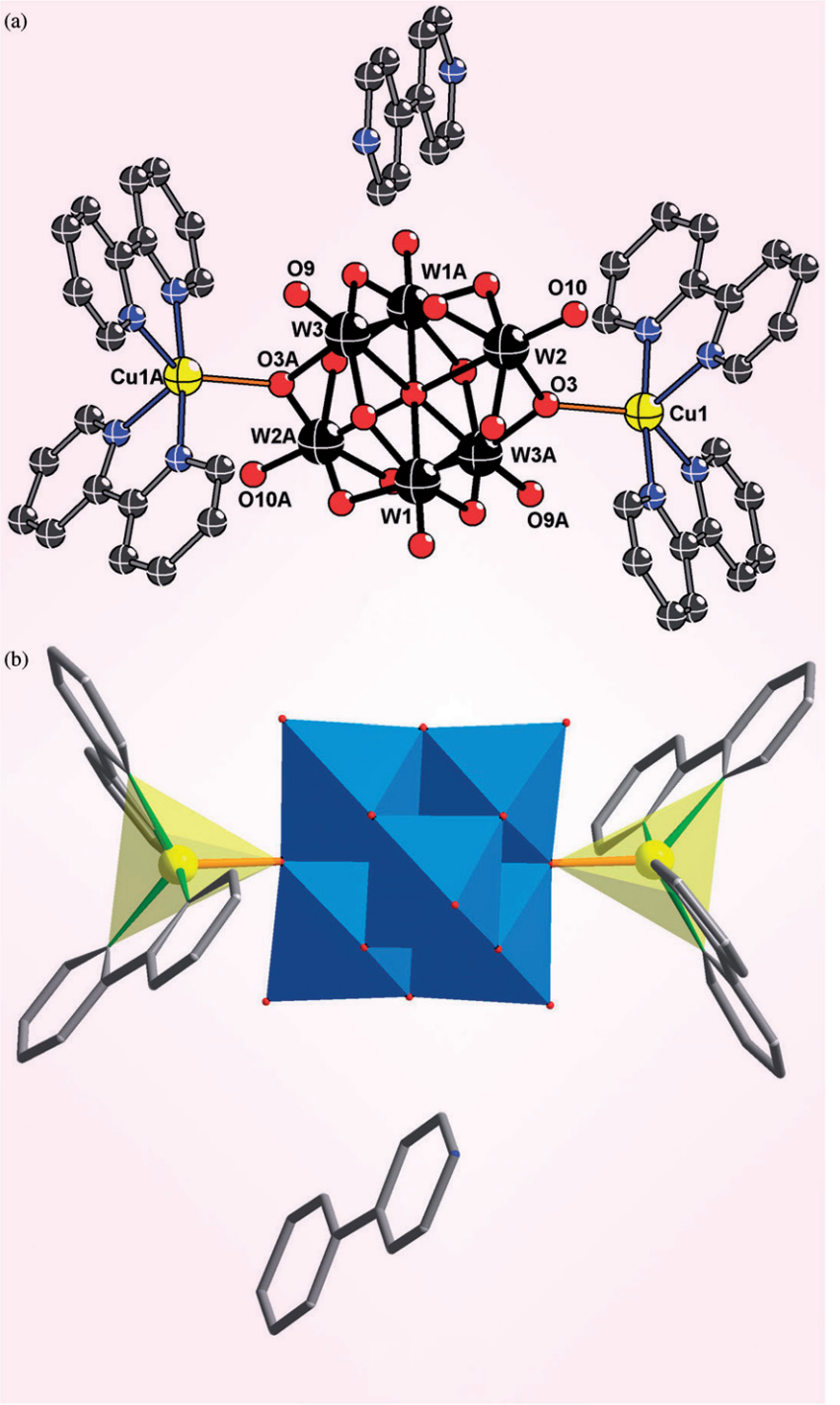

Figure 1. (a) Ball-and-stick representation of **1**. All hydrogen atoms are omitted for clarity. Color codes (online): W (black), Cu (yellow), C (grey), N (blue) and O (red); (b) Polyhedral and ball-and-stick representation of **1**. Color codes (online): $\{CuON_4\}$, yellow polyhedron; $\{WO_6\}$, blue octahedron; C (grey), N (blue) and O (red) atoms are shown with thick sticks.

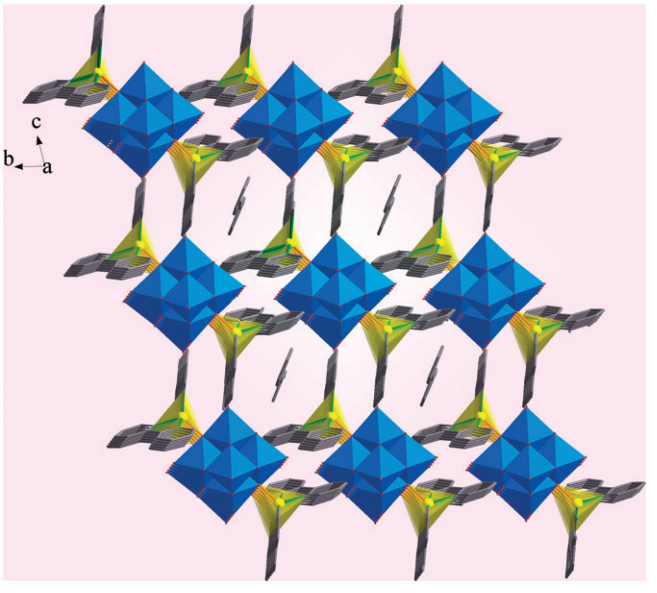

Figure 2. 3-D packing arrangement of **1** viewed along the *a* axis. All hydrogen atoms are omitted for clarity. Color codes (online): {$CuON_4$}, yellow polyhedron; {WO_6}, blue octahedron, C (grey), N (blue) and O (red) atoms are shown with thick sticks.

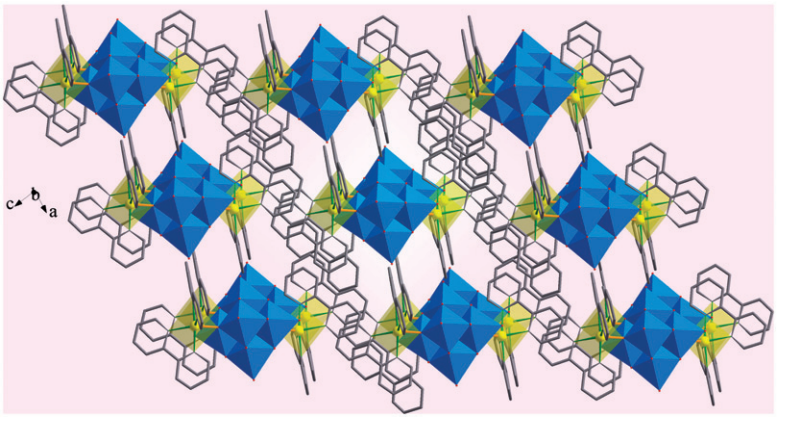

Figure 3. 3-D packing arrangement of **1** viewed along the *b* axis. The polyanions are represented with polyhedra: {$CuON_4$}, yellow polyhedron; {WO_6}, blue octahedron; C (grey), N (blue) and O (red) atoms are shown with thick sticks (color online only).

sodium cations coordinated to the three metal centers via oxygen atoms (see figure 4). There are only a few reports on structures of high-valent manganese-substituted sandwich-type POMs [16]. The polyanion in **2** is charge-balanced by protonated pyridine-4-carboxylic acid molecules. Two are disordered with the occupancy of 50%, as shown with dashed bonds in figure 4. The oxidation states of As, W and Mn sites were determined based on bond lengths and angles, charge balance consideration and the BVS calculations [15]. Results indicate that all As, W and Mn sites possess +3, +6 and +3 oxidation states, respectively. The BVS calculation value of O33 is 1.30, showing that one terminal OH group could exist in the W19 site with the mode of

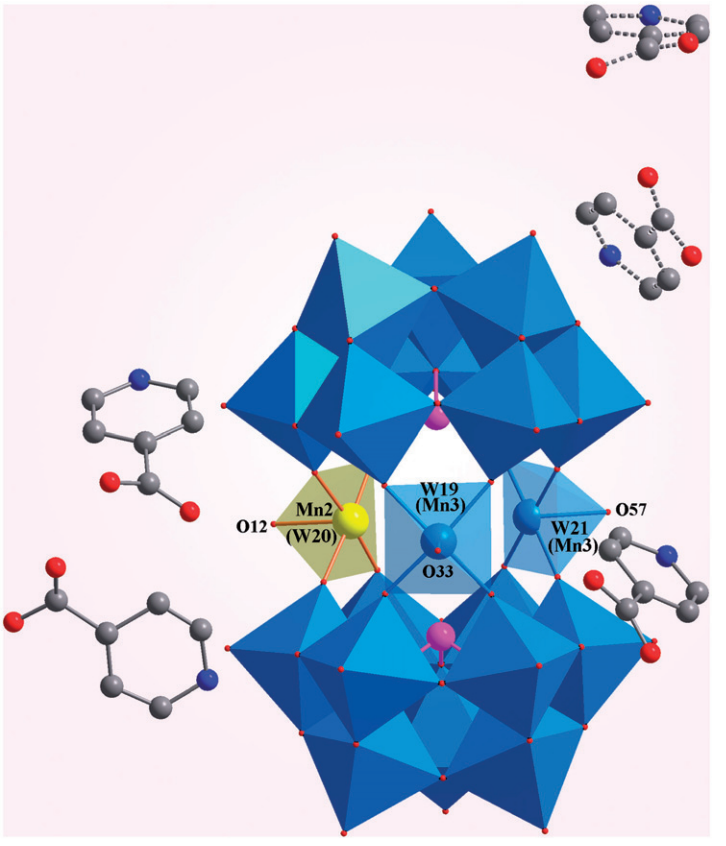

Figure 4. Polyhedral and ball-and-stick representation of **2**. Two of the five pyridine-4-carboxylic acid molecules are disordered with occupancy of 50%, as shown with dashed bonds. Color codes (online): $\{MnO_5\}$, yellow polyhedron; $\{WO_6\}$ and $\{WO_5\}$, blue octahedron; C (grey), N (blue) and O (red) atoms are shown with thick sticks.

{W(OH)}, while O57 has a calculated value of 0.52, representing that one water molecule exists in the W21 site with the mode of $\{W(H_2O)\}$ (see figure 4).

In the packing arrangement, the adjacent dimeric polyanions of **2** are connected by aromatic π–π stacking interactions of pyridine-4-carboxylic acid molecules to form a 3-D open-framework viewed along the *a* axis (see figure 5).

3.3. *FT-IR and UV–Vis spectroscopy*

In the IR spectrum of **1**, the characteristic peaks at 732, 774, 802, 945, 956 and 965 cm^{-1} are ascribed to vibrations of W=O and W–O–W, demonstrating that the polyanion in **1** possesses a Lindqvist structure. The characteristic bands in the region from 1015 to 1609 cm^{-1} can be regarded as features of the 4,4′-bipy and 2,2′-bipy (see figure S3). The IR spectrum of **2** (see figure S4) shows a broad peak at 3438 cm^{-1} and a strong peak at 1725 cm^{-1} attributed to the lattice and coordinated water molecules. The characteristic peaks at 961, 886, 767 and 720 cm^{-1} correspond to ν(As–O), $\nu(W{=}O_d)$, $\nu(W{-}O_b)$ and $\nu(W{-}O_c)$, respectively. The characteristic peaks

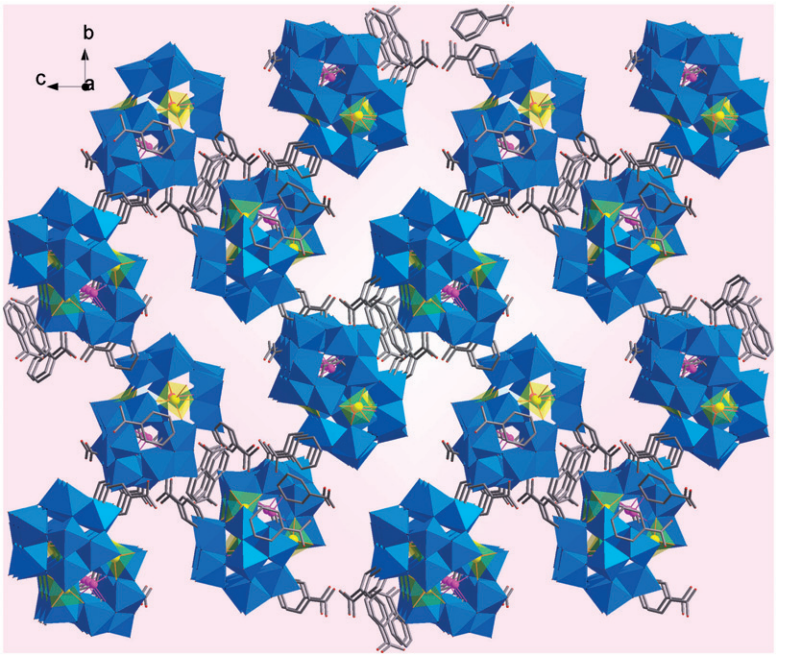

Figure 5. 3-D packing arrangement of **2** viewed along the *a* axis. The polyanions are represented with polyhedra. C, N and O atoms are shown with thick sticks: C (grey), N (blue) and O (red); color online only.

in the region from 1057 to 1606 cm^{-1} can be regarded as features of pyridine-4-carboxylic acid.

The diffuse reflectance UV–Vis spectrum of **1** was also investigated with a solid-state sample in a $BaSO_4$ pellet [see figure 6(a)]. The three peaks at 246, 299 and 363 nm are associated with two kinds of O–W LMCT bands [17a], while the other strong broad band around 778 nm is due to overlap of Cu–N(bipy) and Cu–O(POM) LMCT bands [17b], leading to the dark green color of this compound.

The UV–Vis spectra of **2** are shown in figure 6(b). The insert figure (1 mM in H_2SO_4/Na_2SO_4 with pH = 2.0) shows two strong absorbance bands of **2** (208 nm and 262 nm) between 200 nm and 400 nm, characteristic of charge-transfer bands of terminal and bridging oxygens to tungsten centers, respectively. Figure 6(b) displays the absorbance bands of **2** (5 mM in H_2SO_4/Na_2SO_4 with pH = 2.0) between 400 and 800 nm. The d–d transitions at 501, 531 and 633 nm extend into the visible region, attributed to the $O \rightarrow Mn^{III}$ charge transfer bands.

3.4. *TG and XRPD analyses*

The thermogravimetric (TG) curve of **1** (see figure S5) exhibits the first weight loss of about 6.83% from 225 to 350°C, attributed to loss of non coordinated 4,4′-bipy. This weight loss value is consistent with the calculated one (6.75%). The second weight loss of 26.92% in the temperature range 350 to 650°C corresponds to loss of 2,2′-bipy ligands (Calcd 26.99%). The whole weight loss (33.75%) is in good agreement with the calculated

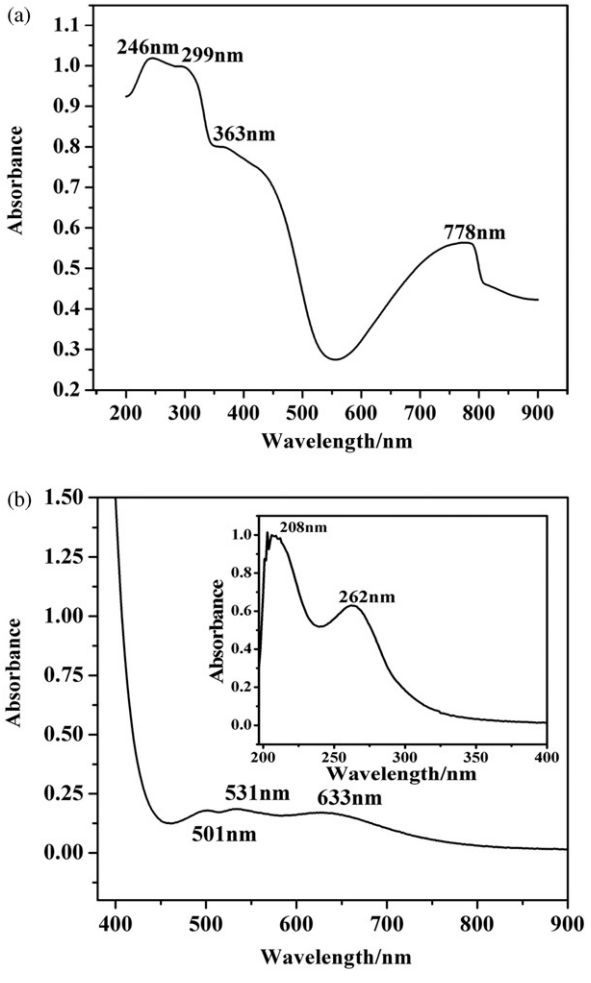

Figure 6. (a) Diffuse reflectance UV–Vis spectrum of **1**; (b) UV–Vis spectrum of **2** recorded with a 5 mM solution in 0.5 M H_2SO_4/Na_2SO_4 at pH = 2.0. Insert: UV–Vis spectrum of **2** in 200–400 nm recorded with a 1 mM solution in 0.5 M H_2SO_4/Na_2SO_4 at pH = 2.0.

value (33.74%), indicating that the result of TG analysis agrees with that of the structure determination.

The TG curve of **2** (see figure S6) shows the first weight loss of ca 6.18% in the temperature range 50 ~ 320°C, corresponding to the loss of all lattice and coordinated water in **2**. This value accords with the calculated value of 6.15%. The second weight loss of 8.40% in the range 350 ~ 455°C is assigned to loss of all pyridine-4-carboxylic acid molecules (calculated 8.48%). The third weight loss step of ca 2.49% in the range 500 ~ 600°C might be partial loss of arsenic oxide from the residue.

In order to check the phase purity of the open frameworks of **1** and **2**, X-ray powder diffraction (XRPD) patterns of **1** and **2** were recorded at r.t. As shown in figure 7, the peak positions of simulated [see figure 7(a)] and experimental [see figure 7(b)] patterns of **1** are in agreement with each other, indicating good phase purity of **1**. Figures 7c and 7d show that the peak positions of both simulated and experimental patterns of **2** accord well

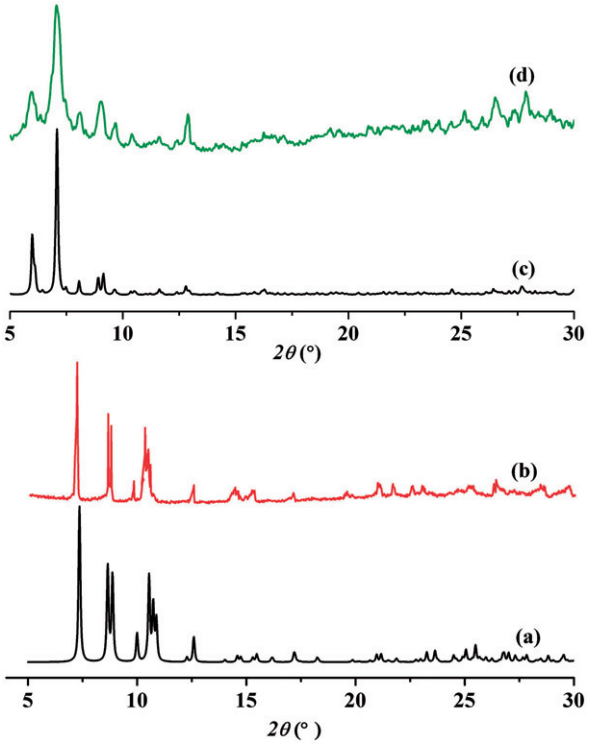

Figure 7. Simulated and experimental XRPD patterns: (a) simulated XRPD of **1**; (b) experimental XRPD of **1** at r.t.; (c) simulated XRPD of **2**; (d) experimental XRPD of **2** at r.t.

with each other, demonstrating that **2** also exhibits good phase purity. The differences in intensity may be due to the preferred orientation of the crystalline powder samples.

3.5. *X-ray photoelectron spectra*

X-ray photoelectron spectra (XPS) were performed to identify the oxidation states of Cu centers in **1** and Mn center in **2**. The XPS for **1** [see figure 8(a)] shows the peaks of *ca*. 953.8 and ca 934.1 eV in the energy region of Cu4p1/2 and Cu4p3/2, confirming that all the Cu centers exhibit the +1 oxidation state [18]. XPS for **2** [see figure 8(b)] display a peak of ca 654.4 eV in the energy region of Mn2p3/2 and a peak of *ca*. 642.4 eV in the energy region of Mn2p1/2, consistent with Mn^{III} oxidation state [19]. These results are in accord with the BVS calculations.

3.6. *Electrochemical behavior*

The cyclic voltammogram (CV) and UV–Vis spectrum of **2** recorded in 0.5 M H_2SO_4/Na_2SO_4 at pH = 2.0 are virtually unchanged with time, indicating that this compound is stable in aqueous solutions. $Cs_6Na_4[(\alpha\text{-}AsW_9O_{33})_2WO(H_2O)Mn_2^{II}(H_2O)_2]$ (**3**) was synthesized according to the literature [20] and used to compare the electrochemical behavior of Mn^{2+} with Mn^{3+} in polyoxoanions. The CV of **3** [figure 9(a)] shows a

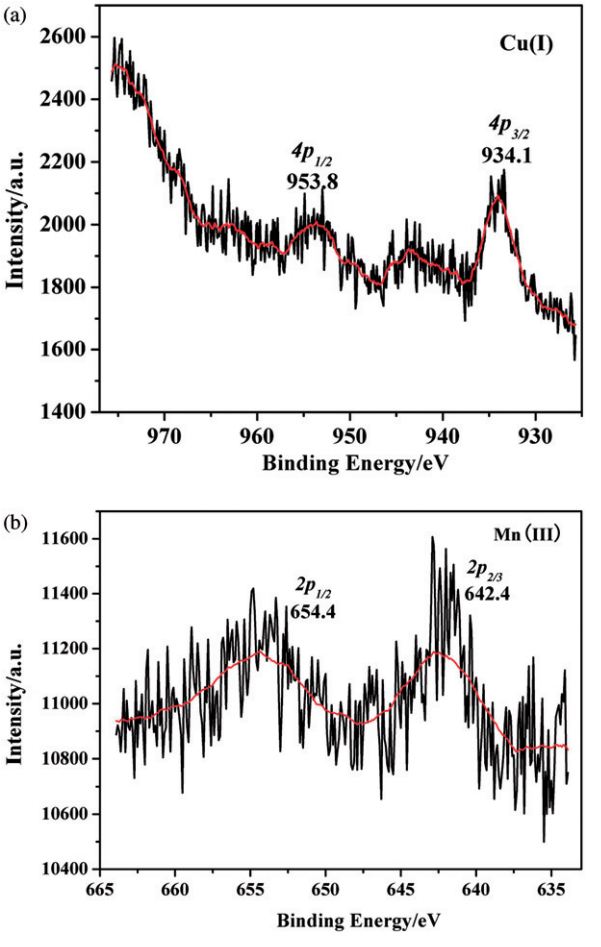

Figure 8. The XPS spectra of (a) Cu(I) in **1** and (b) Mn(III) in **2**.

reversible peak at $E_{1/2} = (E_{pa} + E_{pc})/2 = +801$ mV, indicating the Mn^{II} redox processes and two quasi reversible peaks at $E_{1/2} = -725$ and -507 mV, corresponding to W^{VI} redox processes. Compound **2** [figure 9(b)] shows two similar quasi reversible peaks at $E_{1/2} = -719$ and -510 mV attributed to W^{VI} redox processes, and one blurry and irreversible anodic peak at $+327$ mV which indicates the Mn^{III} redox processes. The blurry redox peaks and irreversible CV feature of **2** probably result from slow electron transfer rather than chemical irreversibility. Compared with the electrochemical behavior of Mn^{2+} in **3**, the anodic peak potential of Mn^{3+} in **2** is much lower, which may be explained by the Jahn–Teller effect existing in high-valent manganese (especially Mn^{III}) -substituted POMs [16a–d].

4. Conclusions

We have synthesized two new organic-inorganic hybrid materials. **1** is a new member in the subfamily of Lindqvist-type compounds and **2** is an organic-inorganic hybrid

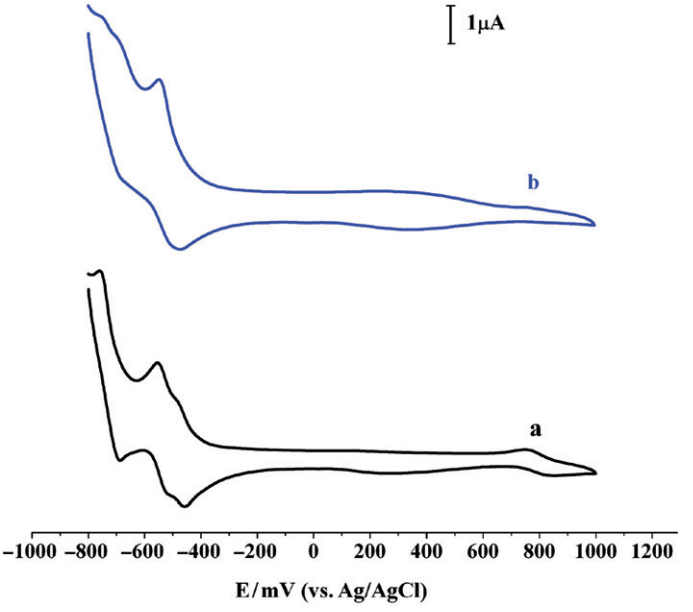

Figure 9. Cyclic voltammograms of (a) **3** and (b) **2** recorded with 1 mM solutions in 0.5 M H_2SO_4/Na_2SO_4 at pH = 2.0. Working electrode: glassy carbon; counter electrode: platinum wire; reference electrode: Ag/AgCl; scan rate: 10 mV s^{-1}.

constructed from a high-valent manganese-substituted sandwich-type POM. The synthesis of these two new compounds shows the feasibility of enriching the POM family by selecting suitable metal ions and organic ligands to modify the POM clusters. Ongoing efforts are focused on the reactions between various functional organic-metal fragments and different types of polyoxoanions to obtain new hybrid materials.

Supplementary materials

Crystallographic data for the structural analysis have been deposited with the Cambridge Crystallographic Data Centre, CCDC reference number: 687369 for **1** and 687370 for **2**. These data can be obtained free of charge at www.ccdc.cam.ac.uk/conts/retrieving.html (or from the Cambridge Crystallographic Data Centre, 12 Union Road, Cambridge CB2 1EZ, UK; Fax: +44-1223/336-033; Email: deposit@ccdc.cam.ac.uk).

Acknowledgements

This work was supported by the National Natural Science Foundation of China (No. 20701005/20701006); the Science and Technology Development Project Foundation of Jilin Province (No. 20060420); the Postdoctoral station Foundation of Ministry of Education (No. 20060200002); the Analysis and Testing Foundation of Northeast

Normal University (NENU); Science and Technology Creation Foundation of NENU (NENU-STC07009) and Science Foundation for Young Teachers of NENU (No. 20070302/20070312); the Program for Changjiang Scholars and Innovative Research Team in University.

References

[1] (a) O.M. Yaghi, H. Li. *J. Am. Chem. Soc.*, **118**, 295 (1996); (b) D. Hagrman, R.C. Haushalter, J. Zubieta. *Chem. Mater.*, **10**, 361 (1998); (c) A.K. Cheetham, G. Férey, T. Loiseau. *Angew. Chem. Int. Ed.*, **38**, 3268 (1999); (d) Z.H. Peng. *Angew. Chem. Int. Ed.*, **43**, 930 (2004); (e) C.L. Hill, (Guest Ed.), *Chem. Rev.*, **98**, 1 (1998); (f) Y.P. Ren, X.J. Kong, X.Y. Hu, M. Sun, L.S. Long, R.B. Huang, L.S. Zheng. *Inorg. Chem.*, **45**, 4016 (2006); (g) J.Y. Niu, Q. Wu, J.P. Wang. *J. Chem. Soc., Dalton Trans.*, 2512 (2002); (h) Z.E. Lin, J. Zhang, J.T. Zhao, S.T. Zheng, C.Y. Pan, G.M. Wang, G.Y. Yang. *Angew. Chem. Int. Ed.*, **44**, 6881 (2005); (i) Y.Q. Sun, J. Zhang, Y.M. Chen, G.Y. Yang. *Angew. Chem. Int. Ed.*, **44**, 5814 (2005).

[2] (a) D.L. Long, E. Burkholder, L. Cronin. *Chem. Soc. Rev.*, **36**, 105 (2007); (b) A. Müller, F. Peters, M.T. Pope, D. Gatteschi. *Chem. Rev.*, **98**, 239 (1998); (c) J.M.C. Juan, E. Coronado. *Coord. Chem. Rev.*, **193**, 361 (1999); (d) P. Mialane, A. Dolbecq, J. Marrot, E. Rivière, F. Sécheresse. *Angew. Chem. Int. Ed.*, **42**, 3523 (2003).

[3] (a) K. Yu, Y.G. Li, B.B. Zhou, Z.H. Su, Z.F. Zhao, Y.N. Zhang. *Eur. J. Inorg. Chem.*, **36**, 5662 (2007); (b) J.W. Zhao, H.P. Jia, J. Zhang, S.T. Zheng, G.Y. Yang. *Chem. Eur. J.*, **13**, 10030 (2007); (c) S.T. Zheng, M.H. Wang, G.Y. Yang. *Chem. Asian J.*, **2**, 1380 (2007); (d) C.Y. Sun, Y.G. Li, E.B. Wang, D.R. Xiao, H.Y. An, L. Xu. *Inorg. Chem.*, **46**, 1563 (2007).

[4] (a) P. Gouzerh, A. Proust. *Chem. Rev.*, **98**, 77 (1998); (b) P. Gouzerh, R. Villanneau, R. Delmont, A. Proust. *Chem. Eur. J.*, **6**, 1184 (2000); (c) C.L. Hill Eds., Special issue on Polyoxometalates, *Chem. Rev.*, **98**, 1 (1998).

[5] (a) H. Jin, C. Qin, Y.G. Li, E.B. Wang. *Inorg. Chem. Commun.*, **9**, 482 (2006); (b) J.Y. Niu, Q. Wu, J.P. Wang. *J. Chem. Soc., Dalton Trans.*, 2512 (2002); (c) J.Q. Sha, J. Peng, A.X. Tian, H.S. Liu, J. Chen, P.P. Zhang, Z.M. Su. *Cryst. Growth Des.*, **7**, 2535 (2007); (d) X.L. Wang, C. Qin, E.B. Wang, Z.M. Su, Y.G. Li, L. Xu. *Angew. Chem. Int. Ed.*, **45**, 7411 (2006); (e) H.Y. An, E.B. Wang, D.R. Xiao, Y.G. Li, Z.M. Su, L. Xu. *Angew. Chem. Int. Ed.*, **45**, 904 (2006); (f) A.X. Tian, Z.G. Han, J. Peng, B.X. Dong, J.Q. Sha, B. Li. *J. Mol. Struct.*, **832**, 117 (2007); (g) H. Jin, X.L. Wang, Y.F. Qi, E.B. Wang. *Inorg. Chim. Acta*, **360**, 3347 (2007); (h) J.Y. Niu, D.J. Guo, J.P. Wang, J.W. Zhao. *Cryst. Growth Des.*, **4**, 241 (2004).

[6] (a) R.G. Cao, S.X. Liu, L.H. Xie, Y.B. Pan, J.F. Cao, Y.H. Ren, L. Xu. *Inorg. Chem.*, **46**, 3541 (2007); (b) V. Shivaiah, M. Nagaraju, S.K. Das. *Inorg. Chem.*, **42**, 6604 (2003); (c) H.Y. An, Y.G. Li, E.B. Wang, D.R. Xiao, C.Y. Sun, L. Xu. *Inorg. Chem.*, **44**, 6062 (2005).

[7] (a) H. Jin, Y.F. Qi, E.B. Wang, Y.G. Li, X.L. Wang, C. Qin, S. Chang. *Cryst. Growth Des.*, **6**, 2693 (2006); (b) H. Jin, Y.F. Qi, E.B. Wang, Y.G. Li, C. Qin, X.L. Wang, S. Chang. *Eur. J. Inorg. Chem.*, **22**, 4541 (2006); (c) T.H. Li, J. Lü, S.Y. Gao, R. Cao. *Inorg. Chem. Commun.*, **10**, 1342 (2007); (d) Y.Q. Lan, S.L. Li, X.L. Wang, K.Z. Shao, Z.M. Su, E.B. Wang. *Inorg. Chem.*, **47**, 529 (2008); (e) J.H. Liao, J.S. Juang, Y.C. Lai. *Cryst. Growth Des.*, **6**, 354 (2006).

[8] (a) L.J. Zhang, Y.G. Wei, C.C. Wang, H.Y. Guo, P. Wang. *J. Solid State Chem.*, **177**, 3433 (2004); (b) V. Shivaiah, S.K. Das. *Inorg. Chem.*, **44**, 7313 (2005); (c) K. Uehara, K. Kasai, N. Mizuno. *Inorg. Chem.*, **46**, 2563 (2007); (d) F. Bannani, R. Thouvenot, M. Debbabi. *Eur. J. Inorg. Chem.*, **27**, 4357 (2007); (e) J. Ping Wang, H. Yu Niu, J.Y. Niu. *Inorg. Chem. Commun.*, **11**, 63 (2008); (f) Z.M. Zhang, J. Liu, E.B. Wang, C. Qin, Y.G. Li, Y.F. Qi, X.L. Wang. *Dalton Trans.*, 463 (2008); (g) J.P. Wang, X.D. Du, J.Y. Niu. *Chem. Lett.*, **12**, 1408 (2006); (h) A. Dolbecq, J.D. Compain, P. Mialane, J. Marrot, E. Rivière, F. Sécheresse. *Inorg. Chem.*, **47**, 3371 (2008).

[9] C. Tourné, A. Revel, G. Tourné, M. Vendrell. *C. R. Acad. Soc. Paris, Ser. C*, **t277**, 643 (1973).

[10] (a) G.M. Sheldrick. *SHELXL-97*, *Program for Crystal Structure Refinement*, University of Göttingen, Germany (1997); (b) G.M. Sheldrick. *SHELXS-97*, *Program for Crystal Structure Solution*, University of Göttingen, Germany (1997).

[11] (a) M. Yuan, Y.G. Li, E.B. Wang, C.G. Tian, L. Wang, C.W. Hu, N.H. Hu, H.Q. Jia. *Inorg. Chem.*, **42**, 3670 (2003); (b) D.Q. Chu, J.Q. Xu, L.M. Duan, T.G. Wang, A.Q. Tang, L. Ye. *Eur. J. Inorg. Chem.*, **5**, 1135 (2001).

[12] (a) J. Gopalakrishnan. *Chem. Mater.*, **7**, 1265 (1995); (b) D. Hagrman, C. Sangregorio, C.J. O'Connor, J. Zubieta. *J. Chem. Soc., Dalton Trans.*, 3707 (1998).

[13] (a) J. Gopalakrishnan. *Chem. Mater.*, **7**, 1265 (1995); (b) S.H. Feng, R.R. Xu. *Acc. Chem. Res.*, **34**, 239 (2001); (c) L.M. Zheng, T. Whitfield, X. Wang, A.J. Jacobson. *Angew. Chem. Int. Ed.*, **39**, 4528 (2000);

(d) P.R. Hagrman, R.L. LaDuca, H.J. Koo, R. Rarig, R.C. Haushalter, M.H. Whangbo, J. Zubieta. *Inorg. Chem.*, **39**, 4311 (2000); (e) P.J. Hagrman, D. Hagrman, J. Zubieta. *Angew. Chem., Int. Ed.*, **38**, 2638 (1999); (f) E. Burkholder, V. Golub, C.J. O'Connor, J. Zubieta. *Inorg. Chem.*, **42**, 6729 (2003).
[14] D. Drewes, M. Piepenbrink, B. Krebs. *J. Cluster Sci.*, **17**, 361 (2006).
[15] I.D. Brown, D. Altermatt. *Acta Crystallogr.*, **B41**, 244 (1985).
[16] (a) X.Y. Zhang, M.T. Pope, M.R. Chance, G.B. Jameson. *Polyhedron*, **14**, 1381 (1995); (b) X.Y. Zhang, C.J. O'Connor, G.B. Jameson, M.T. Pope. *Inorg. Chem.*, **35**, 30 (1996); (c) J.F. Liu, F. Ortega, M.T. Pope. *J. Chem. Soc., Dalton Trans.*, 1901 (1992); (d) X.Y. Zhang, C.J. O'Connor, G.B. Jameson, M.T. Pope. *Polyhedron*, **15**, 917 (1996); (e) P. Mialane, C. Duboc, J. Marrot, E. Riviere, A. Dolbecq, F. Secheresse. *Chem. Eur. J.*, **12**, 1950 (2006); (f) D. Drewes, M. Piepenbrink, B. Krebs. *J. Cluster Sci.*, **17**, 361 (2006).
[17] (a) M.T. Pope. *Heteropoly and Isopoly Oxometalates*, Springer-Verlag, Berlin (1983); (b) B. DasGupta, C. Katz, T. Israel, M. Watson, L. Zompa. *Inorg. Chim. Acta*, **292**, 172 (1999).
[18] (a) C.C. Chusuei, M.A. Brookshier, D.W. Goodman. *Langmuir*, **15**, 2806 (1999); (b) J. Morales, J.P. Espinos, A. Caballero, A.R. Gonzalez-Elipe, J.A. Mejias. *J. Phys. Chem. B*, **109**, 7758 (2005).
[19] Y.F. Han, F.X. Chen, Z.Y. Zhong, K. Ramesh, L.W. Chen, E. Widjaja. *J. Phys. Chem. B*, **110**, 24450 (2006).
[20] U. Kortz, N.K. Al-Kassem, M.G. Savelieff, N.A. Al Kadi, M. Sadakane. *Inorg. Chem.*, **40**, 4742 (2001).